Twelfth Australasian Fluid Mechanics Conference
The University of Sydney, Australia 1995

TOPOLOGY OF FLOW PATTERNS AND ALIGNMENT OF VORTICITY VECTOR WITH PRINCIPAL STRAIN DIRECTIONS

M.S. Chong
Mechanical and Manufacturing Engineering Department
University of Melbourne
Parkville, Victoria 3052
AUSTRALIA

J. Soria
Mechanical Engineering Department
Monash University
Clayton, Victoria 3168
AUSTRALIA

ABSTRACT

All possible incompressible three-dimensional flow patterns can be classified using the second invariant Q and third invariant R of the velocity gradient tensor. Characteristic features of the flow field are revealed in scatter plots of Q versus R using data from full Direct Numerical Simulations (DNS) of turbulence. In this paper it is shown that other significant features of the data, such as the alignment of the vorticity vector with the rate of strain tensor, can also be revealed by suitable normalisation of Q and R.

INTRODUCTION

There are many papers (see for example Jimenez *et al.* 1993 and Moffatt *et al.* 1994) on the structure of vortical motions using data from numerical computations of turbulence. These vortical structures (referred to as *worms* or *sinews* are usually associated with regions of high enstropy. Studies have also been made of the spatial distribution of regions of high dissipation which do not generally overlap with regions of large enstropy. Attempts have also been made to relate these vortices to typical strained generic vortices, such as the Burgers-type vortex or Ludgren-type vortex. Numerical computations of turbulent flow fields produce vast amount of data. A consistent and efficient method of studying vortical structures and high energy dissipating regions found in these simulations is to classify every point in a three-dimensional flow field using the invariants of the velocity gradient tensor (see Chong *et al.*, 1990). This technique provides an unambiguous method of describing the local topology, i.e. all possible three-dimensional flow patterns, in a flow field. Since regions of high enstropy are regions with *focal* local topology and regions of high dissipation are related to regions with *unstable node/saddle/saddle* local topology (see figure 1 for a description of these flow pattern topologies), a method of studying the characteristics of these structures is to map the local topology of every point in the flow field using the three invariants of the velocity gradient tensor A_{ij}. This technique is described briefly in the next section (for a detailed description see Chong *et al.* 1990 and Soria *et al.* 1993).

LOCAL TOPOLOGY AND CLASSIFICATION OF FLOW PATTERNS

For an observer moving in a non-rotating frame of reference with any particle in a flow field, the flow surrounding the particle can be described in terms of the nine components of the velocity gradient tensor A_{ij}, i.e. the velocity $u_i = A_{ij}x_j$. Hence this topological description is independent of the velocity of the observer. The velocity gradient tensor may be broken up into a symmetric and an anti-symmetric part, i.e. $A_{ij} = \partial u_i/\partial x_j = S_{ij} + W_{ij}$, where $S_{ij} = (\partial u_i/\partial x_j + \partial u_j/\partial x_i)/2$ and $W_{ij} = (\partial u_i/\partial x_j - \partial u_j/\partial x_i)/2$ are the rate-of-strain ten-

sor and the rate-of-rotation tensor respectively. The three invariants of A_{ij} are

$$P = -A_{ii} \quad (1)$$

$$Q = \frac{1}{2}[P^2 - S_{ij}S_{ji} - W_{ij}W_{ji}] \quad (2)$$

$$R = \frac{1}{3}(-P^3 + 3PQ - S_{ij}S_{jk}S_{ki} - 3W_{ij}W_{jk}S_{ki}). \quad (3)$$

For incompressible flow the first invariant P is zero and the second invariant Q and the third invariants R form a space which is divided into various topological classifications (see Chong *et al.* 1990). The curve (which forms a cusp at the origin) dividing solutions with complex eigenvalues from that with real eigenvalues is given by

$$\frac{27}{4}R^2 + Q^3 = 0 \quad (4)$$

The above curve and the possible non-degenerate flow patterns in the $Q-R$ space are illustrated in figure 1.

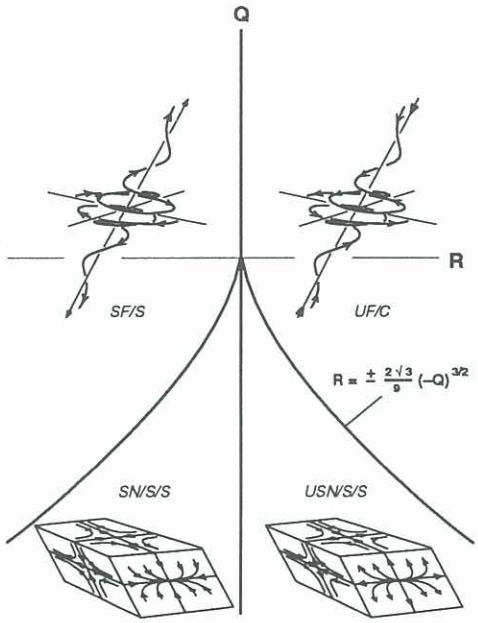

Figure 1: Three dimensional topologies in the $Q-R$ ($P=0$) plane (after Soria *et al.*, 1994)

SF/S: stable focus/stretching,
UF/C : unstable focus/contracting,
SN/S/S : stable node/saddle/saddle, and
USN/S/S : unstable node/saddle/saddle.

Similar expressions can also be obtained for the second and third invariants of the rate of strain tensor (Q_s and R_s respectively) and the rate of rotation tensor (Q_w and R_w respectively). It can be shown that $-Q_s$ is proportional to dissipation and Q_w is proportional to enstropy density.

SCATTER PLOTS OF Q vs R

At a given time step in a numerical computation the second invariant can be plotted versus the third invariant to produce scatter plots. Such scatter plots have revealed significant characteristic feature of a flow field (see Chen *et al.* 1990, Soria *et al.* 1993 and Boratav *et al.* 1995). A example of a scatter plot for a wake flow ($\sim 5 \times 10^5$ data points) is shown in figure 2 (see also Soria & Chong 1993). The scatter plot shows that the bulk of the data lies close to the origin while motions with high gradients lie in the lower right hand quadrant (with *unstable-node/saddle/saddle* topology) or in the upper left hand quadrant (with *stable-focus/stretching* topology).

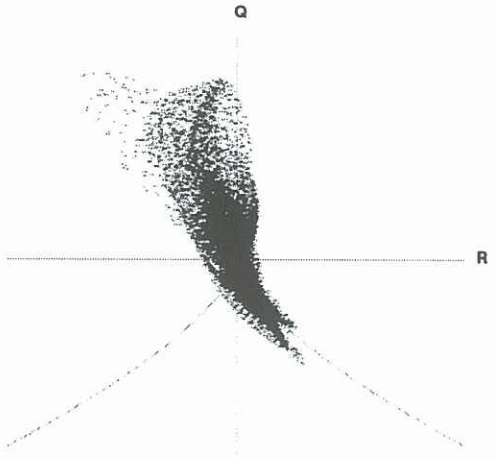

Figure 2: Scatter plot of Q vs R for a wake calculation (see Soria & Chong, 1993)

Other features of a flow field which are important are

- the ratios of the eigenvalues (principal strains) of the rate of strain tensor, and
- the alignment of vorticity vector with the three principal strain directions

(see for example Ashurst *et al.* 1987, Chen *et al.* 1990, Sondergaard *et al.* 1991, Soria *et al.* 1992 and Lund *et al.* 1994). These studies have shown that the vorticity vector is primarily aligned along the eigenvector of the rate of strain tensor which corresponds to the intermediate eigenvalue and that the most probable ratio of the eigenvalues is -3:1:2. This conclusion is generally thought to be contrary to common belief that the vorticity would tend to align with the direction where it is highly stretched, i.e. with the eigenvector corresponding to the highest eigenvalue. However, Majda (1991), Cantwell (1992) and

Boratav *et. al*, using the modified Euler equations (also known as the *simplified/restricted* Euler equations), have shown that there is indeed a tendency for the vorticity to align in the direction of the eigenvector associated with the intermediate eigenvalue. Scatter plots of these analyses have also the same characteristic features as data from DNS of turbulent flow fields.

It would of useful if plots of the second and third invariant of the velocity gradient tensor could also display information regarding the ratio of the eigenvalues of the rate of strain tensor and the alignment of vorticity with the principal strain directions. The eigenvalues (α_i) (with corresponding eigenvector $\mathbf{e}_i$) of the rate of strain tensor can be arranged such that $\alpha_1 \leq \alpha_2 \leq \alpha_3$. For an incompressible fluid, α_1 is always negative, α_3 is always positive and α_2 can be either positive or negative. For a coordinate system aligned with the principal strain directions, it can be shown that the second and third invariants of the velocity gradient tensor are given by

$$Q = -\alpha_2^2 - \alpha_3^2 - \alpha_2\alpha_3 - \frac{1}{4}(\omega_1^2 - \frac{1}{2}\omega_2^2 - \frac{1}{2}\omega_3^2) \quad (5)$$

and

$$R = \alpha_2^2\alpha_3 + \alpha_2\alpha_3^2 + \frac{1}{4}[\alpha_2\omega_1^2 + \alpha_3\omega_1^2 - \alpha_1\omega_2^2 - \alpha_3\omega_3^2] \quad (6)$$

where ω_i are the vorticity components.

Since the local topology at any point in the flow field is governed by the strength of the vorticity field (enstropy) relative to the strength of the strain field, normalised forms of the second invariant Q and third invariant R are $Q^* = Q/|\alpha_i|^2$ and $R^* = R/|\alpha_i|^3$ respectively, where α_i is one of the eigenvalues of the rate of strain tensor (i.e. one of the principal rates of strain).

It can be shown from equations 5 and 6 that

- if the second and third invariant are normalised with the intermediate principal rate of strain, i.e. α_2
- then data points where the vorticity vector is aligned in the direction of the eigenvector corresponding to the intermediate principal rate of strain, will collapse on to a line defined by

$$Q^* - R^* = -1 \quad (7)$$

when α_2 is positive, or to a line defined by

$$Q^* + R^* = -1 \quad (8)$$

when α_2 is negative.

NORMALISED SCATTER PLOTS AND FLOW PATTERN TOPOLOGY

Equations 7 and 8 provides a graphical method of "*displaying*" the alignment of the vorticity vector with the principal strain direction. For the same data as shown in figure 1, plots of the probability of $|cos(\omega, \mathbf{e}_i)|$ have shown that the vorticity vector is primarily aligned with $\mathbf{e}_2$, i.e. the eigenvector corresponding with the intermediate eigenvalue. Hence the plot of Q^* versus R^* for this data would be such that most of the points would lie along the line given by equations 7 and 8. Figure 2 shows the same data given in figure 1 re-plotted with the second and third invariants, Q and R respectively, normalised with α_2. The plot shows distinctly a collapse of the data on lines given by equations 7 and 8 indicating that in the flow field there is indeed a tendency of the vorticity to align in the direction of the intermediate principal rate of strain. Other normalised scatter plots, e.g. for the mixing layer data (Soria *et. al*, 1994), also display the same feature.

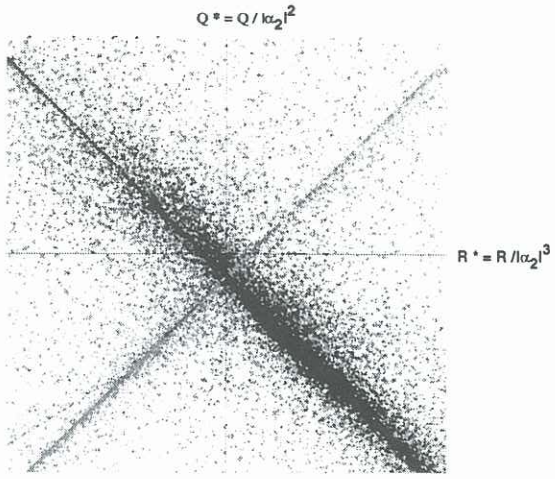

Figure 3: Scatter plot of Q^* vs R^* for same wake data shown in figure 2. Darker points are for α_2 positive and lighter points are for α_2 negative.

Apart form showing the alignment of the vorticity vector with the principal strain directions, the scatter plot also shows the local topology. Unfortunately, although the invariants Q and R (and so will $Q*$ and $R*$) determine the local topology, the flow pattern is not unique and three-dimensional flow patterns are complicated, even for the simple case where the vorticity vector is aligned with one of the principal strain directions. Figure 4 shows the changing local topology for the case where the vorticity vector is aligned with the intermediate strain direction. The flow pattern for the strain field where the ratio of the eigenvalues is -3:1:2 is shown in figure 4(b). There are three orthogonal eigenvector planes which contain solution trajectories and the topologies in the eigenvector planes are *unstable-node/saddle/saddle*. Figure 4(a) shows the location Q^* and R^* as the vorticity is increased in the inter-

mediate strain direction. With vorticity, the eigenvectors e_1 and e_3 are no longer orthogonal and the topologies in the eigenvector planes changes to (c) *unstable-star-node/saddle/saddle* and then to planar flow as shown in (d). The topology in the e_1-e_3 plane which was initially a *saddle* (as shown in (b)) then changes into a *stable-node* and then becomes a *logarithmic node* as shown in (e) and finally to a focus as shown in (f).

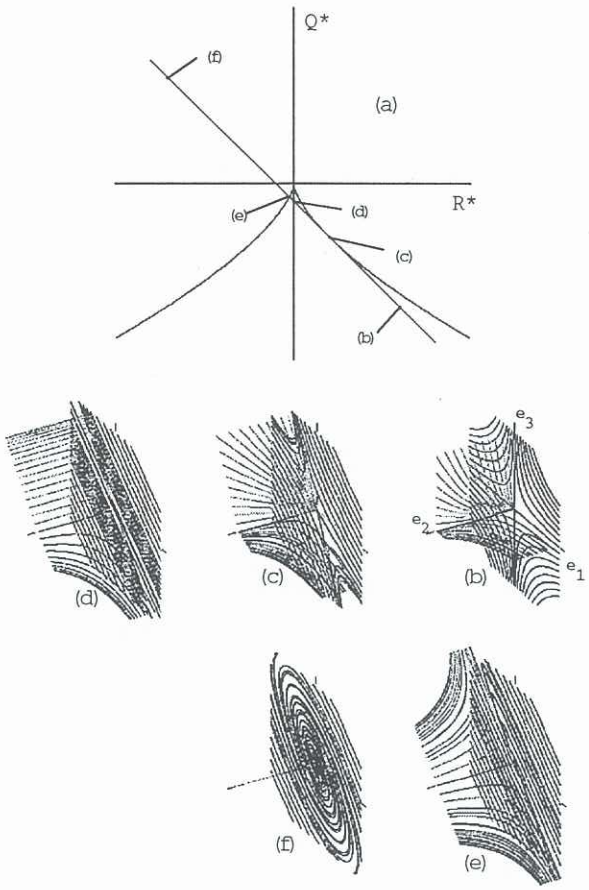

Figure 4: Local topology for a given strain field when the vorticity is increased in the direction of the eigenvector corresponding to the intermediate principal strain direction. The principal strain field is -3:1:2. (a) shows Q^* and R^* for the different flow patterns. (b)-(f) how the local flow pattern for increasing vorticity, where (b) corresponds to the case when the vorticity is zero.

CONCLUSION

This paper describes a method of normalising the second and third invariants of the velocity gradient tensor which collapses the data from a flow field on to lines given by $Q^* \pm R^* = -1$ for points in a flow field where the vorticity vector is aligned with the eigenvector corresponding to the intermediate principal rate of strain. Although the topological classification is relatively easy to determine, the three-dimensional flow pattern is extremely complicated.

REFERENCES

Ashurst, W.T., Kerstein, A.R. Kerr, R.M. & Gibson, C.H. 1987 *Alignment of vorticity and scalar gradient with strain rate in simulated Navier-Stokes turbulence.* Phys. Fluids **25**, 2343-2353.

Boratav, O.N. & Pelz, R.B. 1995 *Locally Isotropic pressure Hessian in a high-symmetry flow.* Phys. Fluids Letters, **7(5)**, 895-897.

Cantwell, B.J. 1992 *Exact solution of a restricted Euler equation for the velocity gradient tensor.* Phys. Fluids A **4(4)**, 782.

Chen, J. Chong, M.S. Soria, J. Sondergaard, R., Perry, A.E. Rogers M., & Cantwell, B. 1990 *A study of the topology of dissipating motions in direct numerical simulations of time-developing compressible and incompressible mixing layers.* CTR Report SS90, NASA Ames Research Center/Stanford University.

Chong, M.S., Perry, A.E. & Cantwell, B.J. 1990. *A general classification of three-dimensional flow fields.* Phys. Fluids **2(5)**, 765-777.

Jimenez, J. Wray, A.A., Saffman, P.G. & Rogollo, R.S. 1993 *The structure of intense vorticity in homogeneous isotropic turbulence.* J. Fluid Mechanics, **225**, 65-90.

Lund, T.S. & Rogers, M.,M. 1994 *An improved measure of strain state probability in turbulent flows.* Phys. Fluids, **6(5)**, 1838-1847.

Majda, A.J. 1991 *Vorticity, Turbulence, and acoustics in fluid flow.* SIAM Review, **33**, 346-388.

Moffatt, H.K., Kida, S. & Ohkitani, K. 1994 *Stretched vortices - the sinews of turbulence; large-Reynolds-number asymptotics.* J. Fluid Mech. **259**, 241-264.

Sondergaard, R., Chen, J., Soria, J. & Cantwell, B. 1991 *Local topology of small scale motions in turbulent shear flows.* 8th Symposium on Turbulent Shear Flows, Munich, Germany.

Soria, J. & Chong, M.S. 1993 *The structure of intense focal regions in a direct numerical wake flow calculation.* 9th Symposium on Turbulent Shear Flows, Kyoto, Japan.

Soria, J., Sondergaard, R., Cantwell, B.J., Chong, M.S. & Perry, A.E. (1994) *A study of the fine-scale motions of incompressible time-developing mixing layers* Phys. Fluids **6(2)**, 871-884.